BOTDA measurements tolerant to non-local effects by using a phase-modulated probe wave and RF demodulation

Javier Urricelqui,* Mikel Sagues, and Alayn Loayssa

Departamento de Ingeniería Eléctrica y Electrónica, Universidad Pública de Navarra Campus Arrosadia s/n, 31006 Pamplona, Spain

**javier.urricelqui@unavarra.es*

Abstract: We demonstrate a Brillouin optical time domain analysis sensor based on a phase-modulated probe wave and RF demodulation that provides measurements tolerant to frequency-dependent variations of the pump pulse power induced by non-local effects. The tolerance to non-local effects is based on the special characteristics of the detection process, which provides an RF phase-shift signal that is largely independent of the Brillouin gain magnitude. Proof-of-concept experiments performed over a 20-km-long fiber demonstrate that the measured RF phase-shift spectrum remains unaltered for large frequency-dependent deformations of the pump pulse power. Therefore, it allows the use of a higher optical power of the probe wave, which leads to an enhancement of the detected signal to noise ratio. This can be used to extend the sensing distance, to improve the accuracy of the Brillouin frequency shift measurements, and to reduce the measurement time.

OCIS codes: (290.5900) Scattering, stimulated Brillouin; (060.2370) Fiber optics sensors; (040.2840) Heterodyne; (999.999) Brillouin distributed sensors; (999.999) Brillouin optical time domain analysis.

References and links

1. M. A. Soto, M. Taki, G. Bolognini, and F. Di Pasquale, "Simplex-Coded BOTDA Sensor Over 120-km SMF with 1-m Spatial Resolution Assisted by Optimized Bidirectional Raman Amplification," IEEE Photon. Technol. Lett. **24**(20), 1823–1826 (2012).
2. X. Angulo-Vinuesa, S. Martin-Lopez, P. Corredera, and M. Gonzalez-Herraez, "Raman-assisted Brillouin optical time-domain analysis with sub-meter resolution over 100 km," Opt. Express **20**(11), 12147–12154 (2012).
3. L. Thévenaz, S. Foaleng Mafang, and J. Lin, "Impact of pump depletion on the determination of the Brillouin gain frequency in distributed fiber sensors," Proc. SPIE **7753**, 775322 (2011).
4. Y. Dong, L. Chen, and X. Bao, "System optimization of a long-range Brillouin-loss-based distributed fiber sensor," Appl. Opt. **49**(27), 5020–5025 (2010).
5. A. Minardo, R. Bernini, L. Zeni, L. Thévenaz, and F. Briffod, "A reconstruction technique for long-range stimulated Brillouin scattering distributed fibre-optic sensors: Experimental results," Meas. Sci. Technol. **16**(4), 900–908 (2005).
6. R. Bernini, A. Minardo, and L. Zeni, "Long-range distributed Brillouin fiber sensors by use of an unbalanced double sideband probe," Opt. Express **19**(24), 23845–23856 (2011).
7. A. Zornoza, M. Sagues, and A. Loayssa, "Self-heterodyne detection for SNR improvement and distributed phase-shift measurements in BOTDA," J. Lightwave Technol. **30**(8), 1066–1072 (2012).
8. J. Urricelqui, A. Zornoza, M. Sagues, and A. Loayssa, "Dynamic BOTDA measurements based on Brillouin phase-shift and RF demodulation," Opt. Express **20**(24), 26942–26949 (2012).
9. A. Zadok, Y. Antman, N. Primerov, A. Denisov, J. Sancho, and L. Thévenaz, "Random-access distributed fiber sensing," Laser Photon. Rev. **6**(5), L1–L5 (2012).
10. K. Hotate and T. Hasegawa, "Measurement of Brillouin gain spectrum distribution along an optical fiber using a correlation-based technique-Proposal, experiment and simulation," IEICE Trans. Electron. E **83**, 405–411 (2000).
11. A. Zornoza, D. Olier, M. Sagues, and A. Loayssa, "Brillouin distributed sensor using RF shaping of pump pulses," Meas. Sci. Technol. **21**(9), 094021 (2010).
12. W. Li, X. Bao, Y. Li, and L. Chen, "Differential pulse-width pair BOTDA for high spatial resolution sensing," Opt. Express **16**(26), 21616–21625 (2008).

13. M. Horowitz, A. R. Chraplyvy, R. W. Tkach, and J. L. Zyskind, “Broad-Band Transmitted Intensity noise induced by Stokes and Anti-stokes Brillouin Scattering in Single-Mode fibers,” IEEE Photon. Technol. Lett. **9**(1), 124–126 (1997).

1. Introduction

Distributed optical fiber sensors are an important field of research and development due to their diverse applications in several industrial sectors. In this context, Brillouin optical time domain analysis (BOTDA) sensors are a mature technology, capable of monitoring temperature and strain over an extended distance range [1] with high spatial resolution [2].

However, the steady increase in the monitoring distance promotes the emergence of a limitation known as non-local effects. These result from the accumulated energy transferred between the probe wave and the pump wave due to stimulated Brillouin scattering (SBS) interaction along the optical fiber. As a result, the pump pulse power is modified depending on the frequency difference between both waves, leading to a deformation of the recovered Brillouin spectrum. Therefore, the accuracy of the temperature or strain measurement given by the Brillouin frequency shift (BFS) is impaired at the last locations of the fiber [3].

Different reports have focused on this effect trying to reduce it. A first solution is to limit the probe wave optical power in order to avoid non-local effects. This limit can be found theoretically or experimentally by evaluating the relation between the biasing effect at the measured BFS and the probe wave optical power [3, 4]. However, setting a maximum power injected into the fiber restricts the signal to noise ratio (SNR) of the measurement, which limits the performance of the sensor. Another proposal is based on a numerical correction system that reconstructs the BFS profile [5]. Nevertheless, this adds complexity to the setup and increases the processing time. Finally, a system with a double probe wave is used to reduce the accumulated energy at the pump pulse wave on its propagation along the fiber [6]. However, this is limited to a particular configuration of the BOTDA sensor and cannot be used in setups using a single probe wave. Therefore, the challenge to perform measurements tolerant to distortions of the pump wave power is still faced by BOTDA sensors.

Recently, we proposed a BOTDA sensor based on self-heterodyne detection that enhances the SNR in relation to the conventional direct detection scheme [7]. Moreover, a dynamic BOTDA sensor based on the Brillouin phase-shift capable of performing measurements largely immune to attenuation in the optical fiber was also demonstrated [8]. In this paper, we propose an improved setup that is able to perform measurements tolerant to non-local effects. Consequently, the probe wave optical power injected into the fiber can be increased resulting in measurements with higher SNR, so that the performance of the sensor is enhanced.

2. Fundamentals

In a conventional BOTDA setup, a probe wave and a pump wave are counterpropagated through an optical fiber with a frequency difference near the BFS (~10.8 GHz for a standard single-mode fiber). As a result, the pump pulse generates a local Brillouin gain or loss (depending on the sensor’s configuration) in the probe wave, whose magnitude depends on the pump pulse power. The spectrum of this interaction, and hence the BFS, can be measured by scanning the frequency difference between the two waves as the probe wave is detected. However, the pump pulse is also affected by SBS interaction, either being slightly amplified (loss configuration) or attenuated (gain mode) at each location of the fiber. Therefore, as the pulse propagates along the fiber, this energy transfer is accumulated and can significantly modify the pulse power, as it is schematically depicted in Fig. 1. More specifically, this amplification of the pump pulse power changes with the frequency difference between the two waves. Therefore, the gain or loss spectrum is scanned with different pump pulse powers, which can distort the recovered spectrum, particularly at the final locations of the fiber ($z \rightarrow L$). This is a non-local effect as the measurement at a particular location is affected by Brillouin interaction at all the preceding locations along the fiber.

This fact is a major restriction for long-range sensing because, as the probe wave optical power increases to achieve larger monitoring distances, the energy transfer between the pump pulse and the probe wave is greater at each location of the fiber and hence, non-local effects become more detrimental.

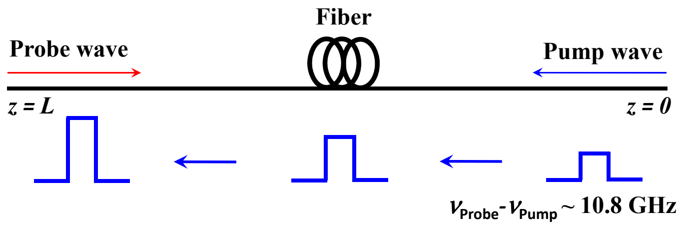

Fig. 1. Schematic representation of the amplification of the pump pulse along its propagation at a conventional loss-based BOTDA sensor.

In contrast to conventional BOTDA sensors, we propose a configuration scheme based on the RF phase-shift [8]. This is shown in Fig. 2, where a phase-modulated probe wave is introduced in one end of an optical fiber while a pump pulse is injected at the other end. This probe wave interacts with the pump pulse via stimulated Brillouin scattering and is directed to the receiver using a circulator. Considering that SBS interaction only affects the first sideband of the modulation, the optical field at the input of the photodetector coming from the interaction between the pump and probe waves at a particular location in the fiber, z, is given by the following expression:

$$\begin{aligned} E(t) = -E_{SB}\exp(j2\pi(\nu_0 - f_{RF})t) + E_0\exp(j2\pi\nu_0 t) \\ +E_{SB}\exp(j2\pi(\nu_0 + f_{RF})t)H_{SBS}(\nu_0 + f_{RF}, z) \end{aligned} \tag{1}$$

where E_0 and E_{SB} are the amplitudes of the optical fields of the carrier and sidebands of the phase-modulated probe wave (higher-order sidebands were neglected, assuming a small modulation index), ν_0 is the optical frequency of the carrier, f_{RF} is the modulation frequency and H_{SBS} is the complex Brillouin loss spectrum at position z, which can be written as:

$$H_{SBS}(\nu, z) = \exp\left(\frac{-g_0\Delta\nu_B}{\Delta\nu_B + 2j\left(\nu + \nu_P - \nu_B(z)\right)}\right) \tag{2}$$

where g_0 is the local gain, $\Delta\nu_B$ is the Brillouin linewidth, ν_B is the Brillouin frequency shift at position z and ν_P is the optical frequency of the pump wave. Note that the proposed system is described for a loss-based sensor but it equally applies for a gain configuration.

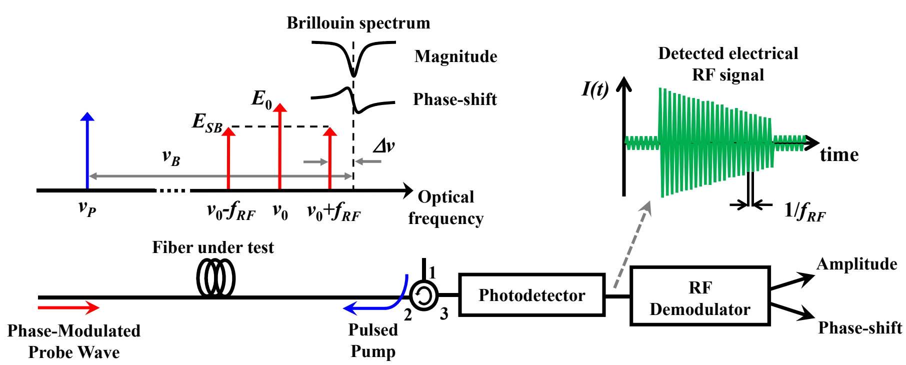

Fig. 2. Schematic representation of SBS interaction and the received RF signal.

The resultant RF signal after detection of the optical field in Eq. (1) can be described in phasorial form by [8]:

$$\begin{aligned} I\big|_{f_{RF}} &= R_D\sqrt{P_0 P_{SB}}\left(H_{SBS}\left(\nu_0+f_{RF},z\right)-1\right) \\ &\approx \frac{R_D g_0\sqrt{P_0 P_{SB}}\Delta\nu_B}{\sqrt{\Delta\nu_B{}^2+4\Delta\nu^2}}\exp\left(-j\arctan\left(2\frac{\Delta\nu}{\Delta\nu_B}\right)\right) \end{aligned} \tag{3}$$

where P_0 and P_{SB} are the optical powers of carrier and modulation sidebands, R_D is the responsivity of the photodetector and $\Delta\nu = \nu_0 + f_{RF} - \nu_B(z) + \nu_P$ is the detuning of the interacting sideband from the center of the Brillouin spectrum. The approximation for the last term has been obtained considering a small g_0.

Notice in Eq. (3) that the detected RF phase-shift is independent of the particular local gain associated to SBS process. As a consequence, it does not depend on the pump pulse power. This feature has major implications regarding the tolerance of the technique to non-local effects as the measurements of the RF phase-shift are not going to be affected by frequency-dependent changes of the pump pulse power.

In order to study theoretically the potential of the technique, we consider the worst case scenario for non-local effects. This arises when a long sensing fiber with a uniform BFS profile is followed by a short section at the far end of the fiber, where the BFS is shifted from the rest of the fiber by $\Delta\nu_B/3$ [3]. As the pump pulse propagates along the fiber, it is amplified by the energy transferred from the probe wave. This amplification of the pump pulse is usually described as a gain factor, which has a direct dependence on the injected probe power into the fiber and the properties of the fiber itself, but not on the injected pump pulse power [3]. In order to present general results independent of the particular parameters of a system, we consider the effects of different gain factors at the end of the long fiber section. These are shown in Fig. 3, where gain factors from 0% (no change of the pump pulse power) to a maximum amplification of 171.8% have been represented. Notice that the pump pulse amplification depends on the frequency difference between pump pulse and probe waves ($\Delta\nu$), following a Lorentzian profile corresponding to SBS interaction. As a consequence, at the last positions of the fiber, the Brillouin spectrum will be scanned deploying a frequency-dependent pump pulse power, resulting in a distorted Brillouin spectrum. This is depicted in Fig. 4(a), where the recovered Brillouin loss spectra at a conventional BOTDA sensor have been calculated considering the frequency-dependent pump pulses of Fig. 3. Arbitrary units are used in the figure, as the focus here is on highlighting the general trends of this effect. As it is shown, the distortion of the measured Brillouin spectrum leads to an impaired accuracy in the measurement of the BFS (Δ_{BFS}). This biasing effect of the peak at the recovered Brillouin loss spectrum can be explained by the increment of the pump pulse power at those frequencies, which generates a higher Brillouin interaction that reduces to a greater extent the magnitude of the probe wave at that location.

In contrast to the conventional BOTDA sensors, if the same conditions are applied to the proposed technique, the recovered RF phase-shift spectra remain unaltered to changes of the pump pulse power. This is highlighted in Fig. 4(b), where the calculated RF phase-shift spectra are superposed independently of the injected probe power. Consequently, larger probe wave power than in conventional BOTDA sensors can be injected into the optical fiber, because the limitation due to non-local effects is mostly removed [3]. This enables a rise in SNR, which could enhance the system performance. Notice that the magnitude of this enhancement depends on the actual noise sources at the particular receiver deployed. For instance, for ideal-shot-noise limited performance, the SNR improvement would be directly proportional to the increment in the detected power. Moreover, this SNR increment adds to that already provided by the RF demodulation deployed in our technique [7]. Therefore, our system enhances the SNR due to two factors: the possibility to inject large probe wave optical powers into the fiber and the demodulation technique.

Finally, we would like to point out that the phase modulation of the probe wave that we deploy in this technique is conceptually different to that used in Brillouin optical correlationdomain analysis sensors, in which both pump and probe waves are modulated so as to synthesize an optical coherence function [9, 10].

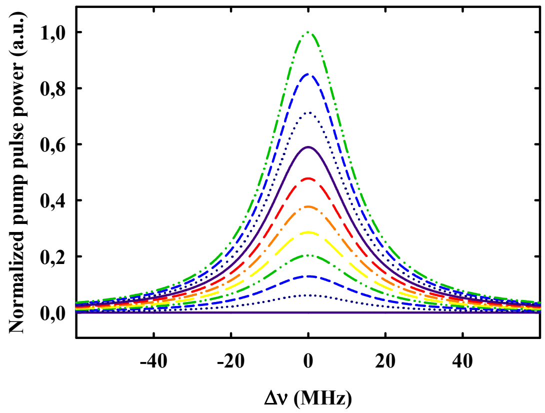

Fig. 3. Normalized pump pulse power as a function of the frequency difference between pump and probe waves, for several probe wave optical powers. A Brillouin interaction with a linewidth equal to 30MHz has been assumed.

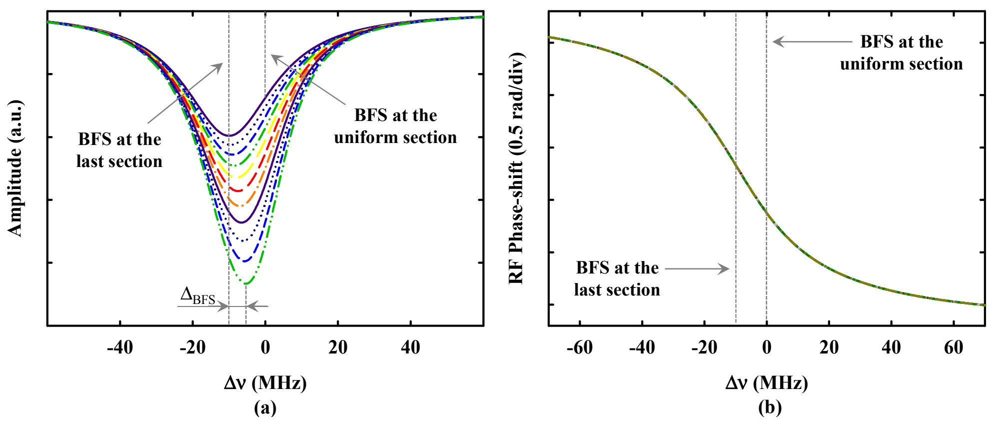

Fig. 4. Calculated (a) amplitude spectra for a conventional loss-based BOTDA and (b) RF phase-shift spectra of the proposed technique for different probe wave powers, at the last section of the fiber.

3. Experimental setup and measurements

The experimental setup depicted in Fig. 5 was assembled in order to validate the capabilities of the technique. The output of a laser source is divided in two optical branches with an optical coupler. In the upper branch, the optical pump pulses are formed using a Mach-Zehnder electro-optic modulator (MZ-EOM) by the RF pulse-shaping technique so as to obtain clean and high extinction ratio pulses [11]. The length of the pulses is set to 50 ns, that is a typical duration for long-range systems based on differential pulse-width pair BOTDA [12], which are the objective of this investigation. The resultant pulse is amplified by an erbium-doped fiber amplifier (EDFA) to obtain an optical power of 21.4 dBm. Before being launched into the sensing fiber via a circulator, its state of polarization is randomized with a polarization scrambler to reduce polarization-mismatching-induced fluctuations on the signal. In the lower branch, a probe wave is generated with an electro-optic phase modulator driven by a 850-MHz RF signal. After interacting with the pump pulses via SBS, the probe signal is directed to a receiver and the resultant RF signal is demodulated. Finally, the BOTDA signal is captured in a digital oscilloscope. Measurements were performed over a 20 km-long standard single-mode fiber, whose last 200 m (the closer to the probe wave input) were introduced in a climatic chamber while the rest of it was maintained at room temperature.

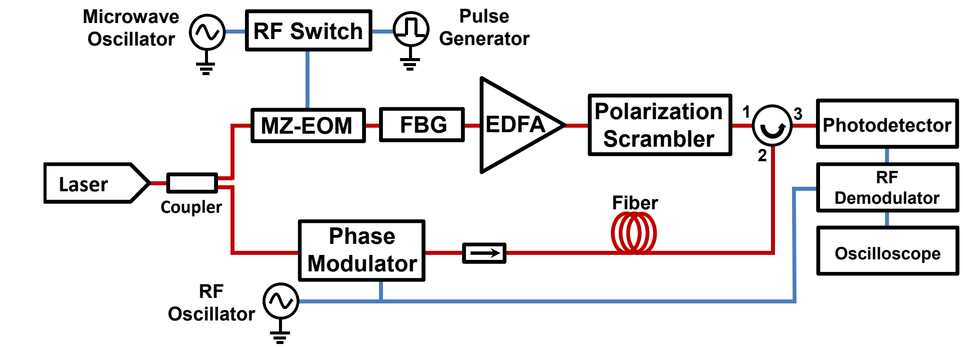

Fig. 5. Experimental setup for the BOTDA sensor based on phase-modulated probe wave and RF demodulation.

In order to determine the amplification suffered by the pump pulse during its propagation through the optical fiber, the pump pulse power was measured for several probe wave powers at the end of the fiber for $\Delta\nu = 0$ MHz. This is depicted in Fig. 6(a), where the measured pulse power is doubled for the largest probe wave optical power in relation to the pump pulse only affected by the attenuation of the fiber. In addition, the pump pulse energy was measured as a function of the frequency difference between the pump and probe waves as shown in Fig. 6(b). Notice the frequency-dependent nature of this amplification as the probe power is increased.

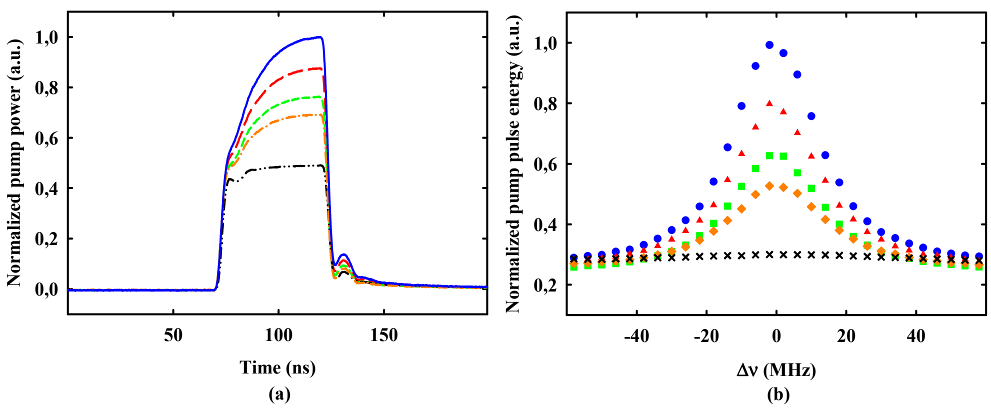

Fig. 6. (a) Measured pulses for different probe wave optical powers (blue solid line 0.67mW, red long-dashed line 0.56mW, green short-dashed line 0.47mW and orange dashed-dot line 0.37mW) and without Brillouin interaction (black dashed-dot-dot line). (b) Measured pump pulse energy at the end of the fiber for several probe wave powers (blue circle symbol 0.67mW, red triangle symbol 0.56mW, green square symbol 0.47mW and orange diamond symbol 0.37mW) and without Brillouin interaction (black cross symbol).

This energy transfer from the probe wave to the pulsed pump is clearly reflected in the amplitude of the BOTDA trace in Fig. 7. The amplitude of the BOTDA trace depends on the pulse power, which is being amplified through its propagation along the fiber. This amplification compensates the attenuation of the fiber (0.2 dB/km) giving rise to an almost flat BOTDA trace.

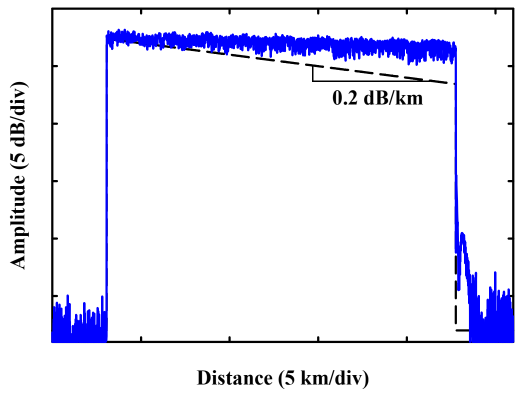

Fig. 7. Measured amplitude of a BOTDA trace at $\Delta\nu = 0$ MHz (blue solid line) and theoretical BOTDA trace not affected by pump wave amplification (black dashed line).

In addition, in order to create a propitious scenario for the emergence of non-local effects, the temperature of the fiber section placed at the climatic chamber was shifted from that of the rest of the fiber [3]. In this situation, measurements of the RF phase-shift and amplitude spectra were performed at the heated section, injecting different probe wave powers into the optical fiber. As it is depicted in Fig. 8(a), the RF phase-shift spectra remain largely independent of probe power in contrast to the amplitude spectra in Fig. 8(b) which are clearly distorted by non-local effects as the probe wave power increases. Note that the maximum power was limited by the onset of SBS pumped by the probe wave itself and seeded by spontaneous Brillouin scattering. This would lead to the addition of noise in the detected signal [13].

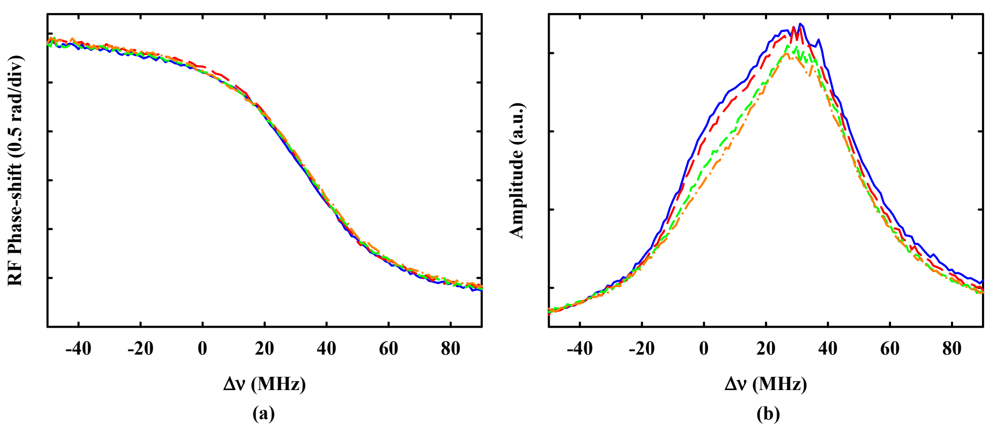

Fig. 8. Measured (a) RF phase-shift spectra and (b) amplitude spectra for different optical powers of the probe wave (blue solid line 0.67mW, red long dashed line 0.56mW, green short dashed line 0.47mW and orange dashed-dot line 0.37mW) at the heated section with a 30°C temperature difference from the rest of the fiber.

Finally, the temperature of the climatic chamber was modified in order to evaluate the performance of the technique for temperature measurements. These measurements were performed setting the probe wave power to a level, which is low enough to avoid spontaneous Brillouin scattering and high enough to induce a large frequency-dependent amplification to the pump pulse. The spectra measured at the heated section of the fiber are depicted in Fig. 9. As it is shown, the RF phase-shift spectra are shifted in frequency as the temperature is risen. However, their shape remains unaltered in contrast to the amplitude spectra, which suffer the detrimental impact of non-local effects. Furthermore, as it is shown in the inset, there is a

#189113 - $15.00 USD Received 19 Apr 2013; revised 7 Jun 2013; accepted 19 Jun 2013; published 11 Jul 2013

good agreement between the changes of temperature at the climatic chamber (5°C per measurement) and the frequency shift of the RF phase-shift spectra. In addition, the BFS corresponding to the RF phase-shift and the amplitude spectra were obtained by performing a mathematical fit based on Eq. (3). This is depicted in Fig. 10, where the linear regression performed to the BFS data obtained from the RF phase-shift spectra shows a clear linear relation with temperature, in contrast to the data obtained from the amplitude spectra.

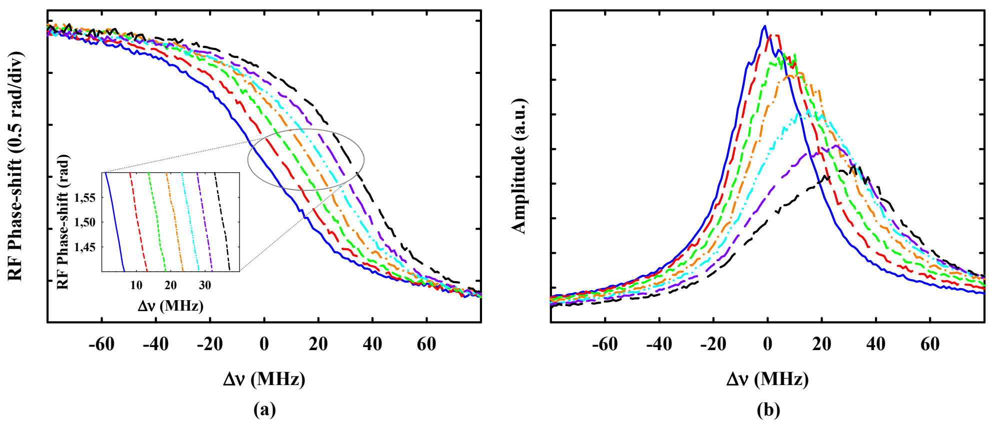

Fig. 9. Measured (a) RF phase-shift spectra and (b) amplitude spectra injecting a 0.67mW probe wave power into the fiber for different temperatures at the climatic chamber from 24°C (blue solid line) to 54°C (black short-long dashed line) in 5°C steps.

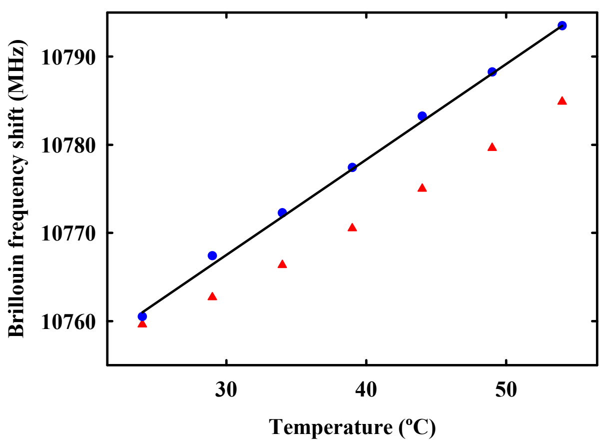

Fig. 10. BFS measurement given by the amplitude spectra (red triangle symbol) and by the RF phase-shift spectra (blue circle symbol). The linear regression to the BFS data obtained from the RF phase-shift (black solid line) gives a 1.08°C/MHz coefficient.

4. Conclusions

We have presented a BOTDA sensor using a phase-modulated probe wave capable of performing measurements tolerant to large frequency-dependent deformations of the pump pulse power. The technique is based on the RF phase-shift spectrum, which is largely immune to variations of the local gain and hence to changes of the pump pulse power. Proof-of-concept experiments have confirmed the theoretical model, as the measured RF phase-shift spectra remained unaltered for large frequency-dependent variations of the pump pulse power, while the amplitude spectra were clearly distorted by non-local effects. Therefore, the proposed system is tolerant to non-local effects overcoming one of the fundamental drawbacks of conventional BOTDA sensors. As a consequence, it is possible to inject higher probe wave optical powers to the sensing fiber in order to enhance the resultant SNR of the measured BOTDA signal. This could be employed to extend the monitoring distance, reduce the measurement time and increase the accuracy of the sensor.

Acknowledgments

The authors wish to acknowledge the financial support from the Spanish Ministerio de Educación y Ciencia through the project TEC2010-20224-C02-01, from the Spanish Ministerio de Economía y Competitividad through the project IPT-2011-12-920000 and from the Universidad Pública de Navarra.